Int. J. Heat Mass Transfer. Vol. 36, No. 8, pp. 2093–2103, 1993
Printed in Great Britain

0017–9310/93 $6.00 + 0.00

Numerical method for direct contact melting in transient process

HIKI HONG and AKIO SAITO
Department of Mechanical Engineering, Tokyo Institute of Technology, O-okayama 2-12-1, Meguro-ku, Tokyo 152, Japan

(*Received* 13 *July* 1992 *and in final form* 8 *October* 1992)

Abstract—Most of the research on direct contact melting has been carried out on the assumption of steady state or quasi-steady state. Such a methodology, however, is difficult to apply to problems in which the boundary conditions such as the temperature of heating plate or the external force exerted on the solid PCM change abruptly with time. In this study, we show an efficient algorithm to solve the transient behavior of direct contact melting, considering the solid movement by external forces exerted on a solid body as well as that by melting. The method is based on the enthalpy method, but is especially devised to satisfy the force balance on solid phase with velocity variation. It is examined through two test problems. The first one is that the system gradually approaches the steady state after the start of melting. The result shows good agreement with that by the previous steady state approach, and it is assured that the behavior during the transient process to steady state is very reasonable in a viewpoint of a physical phenomenon. The second one deals with a rather complicated situation of a copper block above a melting temperature being cooled by ice. It was verified that the present methodology can deal with such a conjugate problem feasibly and simply.

INTRODUCTION

DIRECT contact melting can be observed if a heating plate and a solid PCM are pressed against each other while the solid is being melted and the melted liquid is flowing out through a thin liquid layer. This phenomenon occurs in numerous natural and technological processes, such as metallurgy, welding, geology, nuclear technology and latent thermal storage system. In general, the heat transfer rate during the direct contact melting process is much greater than that in the melting dominated by heat convection which occurs in a relatively thick space between source and solid. Therefore, owing to the practical importance of the subject, there have been a large number of studies to clarify the mechanism of the direct contact melting, particularly on a target of the thermal storage system which usually needs high heat flux in melting process.

Over the past decade, many papers [1–8] were published in this field and the mechanism of heat transfer and the phenomenon of direct contact melting was found out through analytical and experimental investigations. The results show that the predominant effect of heat transfer is mainly the heat conduction in the low range of *Ste* number, but gradually the effect of the convection increases with higher *Ste* number.

Most of the researches through numerical analysis [2, 6, 8] were conducted on the assumption of steady state. Actually, if the melting continues under a constant surface temperature of heating plate and a constant pressure, the system approaches steady state or quasi-steady state, that is, the apparent velocity of the solid phase comes to equal the melting speed and the liquid–solid interface does not move in space, as long as the inertia term in the force balance equation for solid phase can be neglected. Experimental investigations clarified the validity for such an assumption.

Nevertheless, the boundary conditions, according to the problems, can be changed remarkably with time. Furthermore, the transient process of melting itself can be the object to be examined. However, the previous steady state approaches have a serious limitation in solving such problems due to a lack of feasibility and flexibility.

To solve a transient process of direct contact melting, the problem should be treated as a kind of moving boundary problem, in which the liquid–solid interface moves with time. Some methods to solve those moving boundary problems associated with phase change have been developed and can be divided into two groups; transformed [e.g. 9, 10] and fixed grids [e.g. 11, 12]. Lacroix and Voller [13] recognized that both transformed and fixed grids can be applied with success to a wide variety of problems and offer powerful means for solving a phase change problem.

The transient behavior during direct contact melting can be characterized by the moving solid phase which is not fixed in space and has a varying velocity with time. Therefore, the moving velocity must be calculated together with other dependent variables. The transformed grids method is apparently an efficient method to solve a phase change problem, but seems to be difficult to apply to the present problem. A vast amount of calculation is required for region transformation; in the transformed grids method, the physical region must be mapped from the real region each time step and in the present work, on account of

NOMENCLATURE

a, b	coefficients, equation (7)
c	specific heat
f	local liquid fraction
g	dimensionless gravity acceleration
H	height of solid phase
h_m	latent heat of fusion
k	thermal conductivity
M	dimensionless mass
p	dimensionless pressure
Pr	Prandtl number, ν/α
q	dimensionless heat transfer rate
R	half width of solid
S_c	source term, equation (7)
Ste	Stefan number, $c(T_w-T_m)/h_m$
t	dimensionless time
T	temperature
u	dimensionless x-velocity
v	dimensionless y-velocity
V	dimensionless moving velocity of solid phase
(vol)	volume of control volume
x, y	dimensionless coordinates.

Greek symbols

α	thermal diffusivity
α_f	relaxation factor of liquid fraction
δ	thickness of liquid layer
θ	dimensionless temperature
μ	viscosity
ρ	density
ϕ	angle of slope.

Subscript

P, N, S, E, W	grid points (Fig. 2)
w	wall
m	melting point
latn	latent heat
sens	sensible heat
cool	heat extracted from copper block
s	solid
l	liquid.

Superscript

–	average
b	base line
k	kth iterate
o	previous time step
s	shifted.

the unknown solid velocity, the calculation domain is in an undetermined state and, consequently, must be recalculated whenever the assumed velocity is updated; even in one time step.

In the enthalpy method (a kind of fixed grids method), it is not necessary to obtain the calculation domain and to transform the physical region to the calculation region. In this paper, we suggest an efficient algorithm to solve the transient behavior of direct contact melting problems, which is based on the enthalpy method, but includes the effect of the moving solid phase.

Finally, we illustrate the usefulness and effectiveness of the algorithm through two test problems; the first one is to solve the geometrically simple system which leads to the steady state and to compare the solution with the solution by the previous method, and the second one is to be associated with the problem that the copper block with an initial temperature T_w is being cooled by the ice. Of course, the surface temperature varies not only with time but also with the location.

FORMULATION

The governing equations appearing in conventional enthalpy methods are usually based on primitive variables with the energy expressed in terms of enthalpy. In nondimensional form, the primitive variable formulation in two-dimensional Cartesian coordinates is

Continuity equation:

$$\frac{\partial u}{\partial x}+\frac{\partial v}{\partial y}=0 \tag{1}$$

Momentum equations:

$$\frac{\partial u}{\partial t}+u\frac{\partial u}{\partial x}+v\frac{\partial u}{\partial y}=Pr\left(\frac{\partial^2 u}{\partial x^2}+\frac{\partial^2 u}{\partial y^2}\right)-\frac{\partial p}{\partial x} \tag{2}$$

$$\frac{\partial v}{\partial t}+u\frac{\partial v}{\partial x}+v\frac{\partial v}{\partial y}=Pr\left(\frac{\partial^2 v}{\partial x^2}+\frac{\partial^2 v}{\partial y^2}\right)-\frac{\partial p}{\partial y} \tag{3}$$

Energy equation:

$$\frac{\partial \theta}{\partial t}+u\frac{\partial \theta}{\partial x}+v\frac{\partial \theta}{\partial y}=\frac{\partial^2 \theta}{\partial x^2}+\frac{\partial^2 \theta}{\partial y^2}-\frac{1}{Ste}\frac{\partial f}{\partial t} \tag{4}$$

scales

time	$R^2\alpha^{-1}$
length	R
velocity	αR^{-1}
pressure	$\rho\alpha^2R^{-2}$
temperature	T_w-T_m

where p represents the dimensionless pressure; u and v are the dimensionless velocities in the directions of

x and y, respectively; θ is the dimensionless temperature; and f is the local liquid fraction. The density and thermal conductivity of the solid phase were regarded as the same as those of the liquid phase.

In the above energy equation, the last term in the right-hand side is related to the change of the liquid fraction or latent heat in a cell. The liquid fraction does not change gradually from the liquid region to the solid region in the present problem. Even though it does not seem to be proper mathematically to express this term like equation (4), we determined to use it as it is, owing to the convenience for numerical calculation.

Though there are several techniques to solve the above momentum equations which correspond to both liquid and solid phase regions, we used the method by Gartling [14], that is, the viscosity in a computational cell is treated as a function of the liquid fraction. In the present work, the harmonic average value of the viscosity weighted by liquid fraction was used.

$$\mu = \frac{1}{f/\mu_l + (1-f)/\mu_s}. \tag{5}$$

By using equation (5), the viscosity (Pr in non-dimensional form) in the solid region is taken as a very large number (1×10^{30}), which makes the velocities in solid region constant and the viscosity in liquid region has its own value. Moreover, in the computational cell mixed with both liquid and solid, the viscosity varies properly with the liquid fraction. In this way, the velocity condition at the liquid–solid interface can be taken into account. We used the algorithm SIMPLEC [15] revised by Van Doormaal as the numerical solver.

The direct contact melting needs one more equation to close the problem, which is the force balance for the solid body (see Fig. 1). The term of the timewise variation of the total mass of solid phase is neglected because it is much less than other terms if not in the range of a very large Ste number.

$$Mg - \bar{p} = M\frac{\mathrm{d}V}{\mathrm{d}t}, \quad \left(\bar{p} = \int_0^l p\,\mathrm{d}x\right) \tag{6}$$

scales

acceleration	$\alpha^2 R^{-3}$
mass per unit depth	ρR^2

where M is a dimensionless mass and also denotes the aspect ratio of the solid phase (H/R); g is a dimensionless gravity acceleration; and V is a dimensionless apparent velocity of solid phase. By solving the above equation on the base of the pressure distribution in the liquid layer, the moving velocity of solid phase can be obtained.

Indeed, the energy equation has a decisive role associated with the timewise movement of the liquid–solid interface in a phase change problem, in particular, in the problem considered here on account of the moving solid phase. The driving factor in the source term in the energy equation is the local liquid fraction f. In a numerical calculation, it is updated iteratively from the solution of the energy equation. The discretization equation of energy can be expressed

$$a_P\theta_P = a_N\theta_N + a_S\theta_S + a_E\theta_E + a_W\theta_W + b$$

$$b = a_P^\circ\theta_P^\circ + S_c\,(\mathrm{vol})_P$$

$$S_c = -\frac{1}{Ste}\frac{f_P^k - f_P^\circ}{\Delta t}$$

$$b = a_P^\circ\theta_P^\circ + \frac{1}{Ste}\frac{f_P^\circ}{\Delta t}(\mathrm{vol})_P - \frac{1}{Ste}\frac{f_P^k}{\Delta t}(\mathrm{vol})_P \tag{7}$$

where the a's denote coefficients relating the point P and its surrounding nodes (see Fig. 2), as frequently appeared in SIMPLE-type method; $(\mathrm{vol})_P$ is the volume of the control volume P; f_P° is the liquid fraction in the previous time step (see Fig. 3(a)); and f_P^k is the liquid fraction at the kth iteration in Pth control volume in the current time step.

From equation (7), it is apparent that the source term S_c is the timewise change of liquid fraction which corresponds to the melting amount in a control volume if the solid does not move. On the other hand, in the problem considered here, the effect of the moving solid body with the varying velocity V must be included and, consequently, a special manipulation should be demanded, which will be explained using Figs. 3(b) and (c).

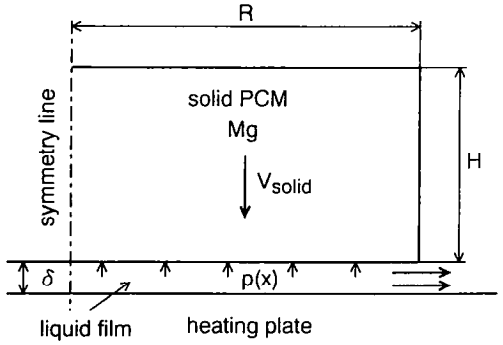

FIG. 1. Schematic diagram of direct contact melting and the force balance for a solid phase body.

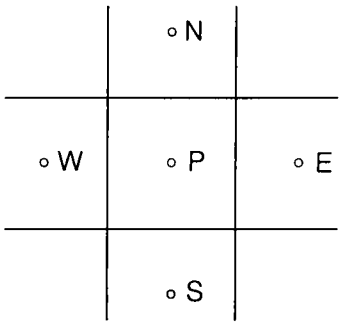

FIG. 2. Location of grid points in control volumes.

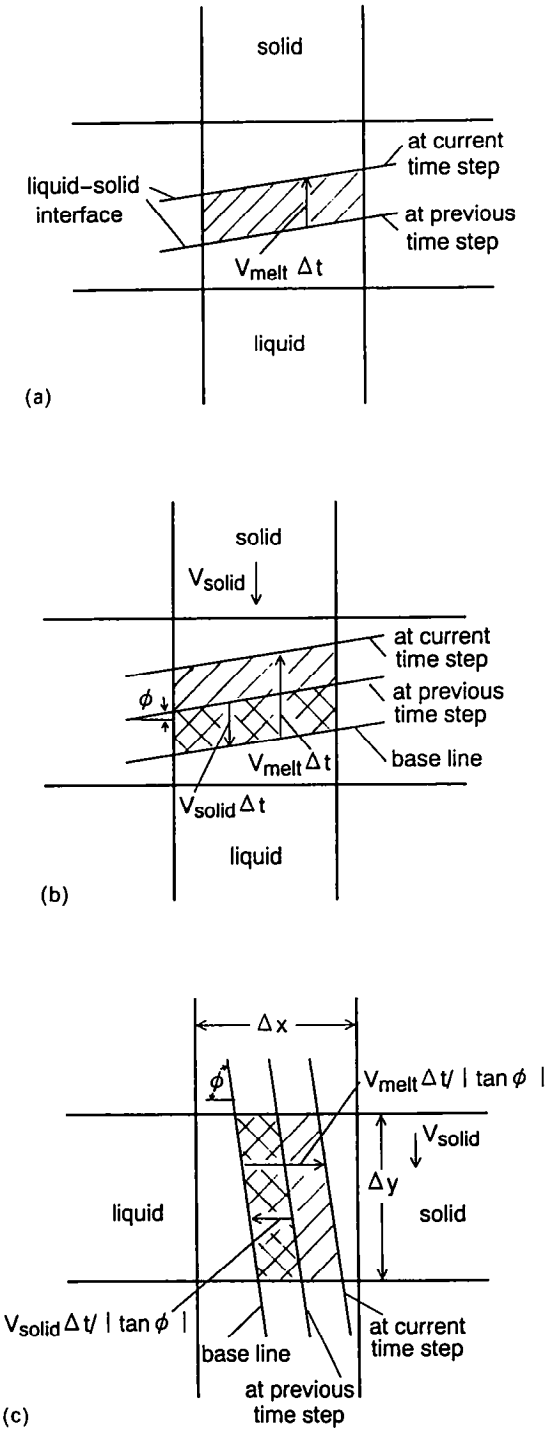

FIG. 3. Sketch showing the movement of the liquid–solid interface in the control volume where the phase change occurs; (a) solid phase fixed in space, (b) solid phase moving with velocity V ($\phi < 45°$), (c) solid phase moving with velocity V ($\phi > 45°$).

As shown in Figs. 3(b) and (c), it is modeled that the liquid–solid interface moves by the distance of $V\Delta t$ ($V_{solid}\Delta t$ in the figures) in the direction of the velocity of the solid body. The melting proceeds on the base of that shifted liquid–solid interface, different from that in the fixed solid problem. Therefore, the liquid fraction at the previous time step f_P^o in equation (7) should be replaced by the base liquid fraction f_P^b, which is defined as

$$f_P^b = f_P^o - f_P^s \tag{8}$$

where f_P^s refers to the cross-hatched region in Figs. 3(b) and (c). For the accurate calculation of f_P^s, the location of the liquid–solid interface within a grid is required. In the present work, it is assumed that the line can be approximated by a straight line cutting through the grid. If the slope is smaller than 45° from the horizontal line (see Fig. 3(b)), the line can be considered to be closer to horizontal than vertical, otherwise closer to vertical (see Fig. 3(c)) [16]. For each case, the value of f_P^s can be approximated as follows:

if $\phi < 45°$

$$f_P^s = \frac{V\Delta t(\Delta x)_P}{(\text{vol})_P} \tag{9}$$

if $\phi > 45°$

$$f_P^s = \frac{V\Delta t(\Delta y)_P/|\tan\phi|}{(\text{vol})_P}.$$

Using equations (8) and (9), the base liquid fraction at the computational cells where the phase change occurs can be calculated. However, the method described above frequently brings about a negative value of f_P^b, which leads to physical violation. Two approaches can be thought of; the one is to be forced to calculate using the negative values and the other is to shift the negative component of f_P^b to the neighbor cell located in the opposite direction to the melting front direction, e.g. the south in Fig. 3(b) and the west in Fig. 3(c):

if $\phi < 45°$

$$f_S^b = 1 + \frac{f_P^b(\text{vol})_P/(\Delta x)_P}{(\Delta y)_S}$$

$$f_P^b = 0 \tag{10}$$

if $\phi > 45°$

$$f_W^b = 1 + \frac{f_P^b(\text{vol})_P/(\Delta y)_P}{(\Delta x)_W}$$

$$f_P^b = 0.$$

The stability and accuracy for each approach were thoroughly examined through the test problems explained later. It was concluded that the latter-shift method is somewhat superior to the former-negative value method from a viewpoint of the stabilized convergence of computation. On the test problem 1 where the liquid layer increases continuously as time proceeds, almost the same results were acquired; but on the test problem 2 where the liquid layer forms its peak in thickness with time and decreases gradually after the peak owing to the reduced surface tem-

perature of the heating plate, the divergence does frequently happen by the former-negative method during the decreasing process of the thickness.

For an assumed or updated solid velocity, the local liquid fraction in control volume P, can be solved iteratively. That is, after the solver returns the $(k+1)$th temperature field, the $(k+1)$th liquid fraction field is updated using equation (11), a rearrangement of equation (7):

$$f_P^{k*} = Ste\,\Delta t/(\mathrm{vol})_P\left(a_N\theta_N + a_S\theta_S + a_E\theta_E + a_W\theta_W + a_P^0\theta_P^0 + \frac{1}{Ste}\frac{f_P^b}{\Delta t}(\mathrm{vol})_P\right)$$

$$f_P^{k+1} = \alpha_f(f_P^{k*} - f_P^k) + f_P^k. \tag{11}$$

The sequence of steps in the important procedure of calculation is:

1. Assume a solid velocity V.
2. Calculate the velocity, pressure and temperature field.
3. Calculate the liquid fraction field from temperature field.
4. Return to step 2 until the proper convergence condition is satisfied.
5. Update the solid velocity V and adjust the base liquid fraction.
6. Return to step 2 with updated solid velocity V. Iterate until the velocity satisfies the force balance (equation (6)).
7. Increase the time step and return to step 2.

At step 5, the instantaneous solid velocity V and the average pressure p along the solid–liquid interface must satisfy equation (6), which can be expressed in terms of V in a difference form

$$V = (g - \tilde{p}/M)\Delta t + V^0. \tag{12}$$

Since the liquid layer is very thin, the pressure field in it is sensitively dependent on the solid velocity. Accordingly, if the average pressure and the solid velocity are underrelaxed with the previous iterative values, so many iterations are needed in order to satisfy the equation of force balance as much as the accuracy of the numerical calculation demands. Such a method has a difficulty in selecting the proper relaxation factors as well. Moreover, even using very small relaxation factors, there does exist a possibility of divergence according to the complexity of the problem.

Therefore, instead of using equation (12), it was used in a modified form.

$$f(V) = (g - \tilde{p}/M)\Delta t + V^0 - V = 0. \tag{13}$$

As a result, the process to obtain the solid velocity V was replaced by finding the root of $f(V)$ in the above equation. Referring to the velocity V^0 at the previous time step, the function $f(V)$ is bracketed in the interval containing the root. As the algorithm to find the root in the present work, the bisection method was used on account of its simplicity and stability.

TEST PROBLEMS

The present numerical methodology is tested for two problems: The first is to evaluate the unsteady behavior in the representative problem often utilized in the field of direct contact melting. The second is a kind of conjugate problem, a rather complicated system consisting of a phase change material and a copper block as a heating plate.

Test problem 1

Problem description. The problem is schematically shown in Fig. 4 with the boundary conditions. The solution by the steady state method is available and can be compared easily with that by the present method.

Initially, the heating plate and the solid phase remain at a constant temperature (the melting point of PCM) and in contact directly without a liquid layer between them. The temperature of the heating plate rises abruptly to T_w and the melting starts.

It is noted that as melting proceeds, the height of the solid phase is reduced and, consequently, the force exerted on the liquid layer becomes smaller and smaller with time. However, though there are no difficulties in including the effect of reducing height in calculation, it is impossible for the system to completely reach steady state and difficult to strictly compare with the result of the conventional steady state solver. Accordingly, we assume that the height of solid phase does not change, in fact, which does not bring about a serious result because the timewise variation of pressure by the height reduction is not so fast under given conditions in this problem.

The calculation was performed in a non-dimensional form, but the phase change material was considered to be an ice and the nondimensional parameters were obtained on the base of the ice. A number of calculations to verify the method presented here were carried out, but it was found that the characteristics are almost the same. Therefore, only two results will be reported here and their conditions are listed in Table 1.

A 15×14 grid was used, spaced uniformly in the y-direction, but spaced partially non-uniformly near the exit region in the x-direction.

Results. Figure 5 for Case A, being enlarged by 200 times in the y-direction, shows the velocity field and the liquid–solid interface at times $t = 8 \times 10^{-6}$, $t = 2 \times 10^{-5}$, and $t = 2 \times 10^{-4}$ (15 s) which cor-

Table 1. Conditions in test problem 1

	Ste	*M*	*Pr*	*g*
Case A	1.266×10^{-2}	1	13.44	5.521×10^{11}
Case B	1.266	10	13.44	5.521×10^{11}

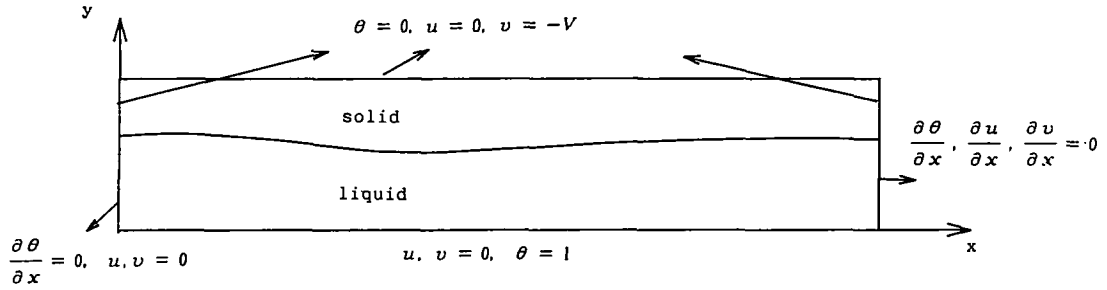

FIG. 4. Sketch of problem 1 and the boundary conditions.

responds to the time when the system completely reaches the steady state. As evidenced in these figures, the liquid–solid interface is utterly linear and parallel to the heating plate. That is an expected phenomenon at lower *Ste* number (usually less than 0.1), in which the dominant effect upon the heat transfer is heat conduction and is well known from previous studies.

Figure 6, being enlarged by 100 times, corresponds to Case B and has almost the same trend to Fig. 5. Though it is impossible to observe visually, the liquid

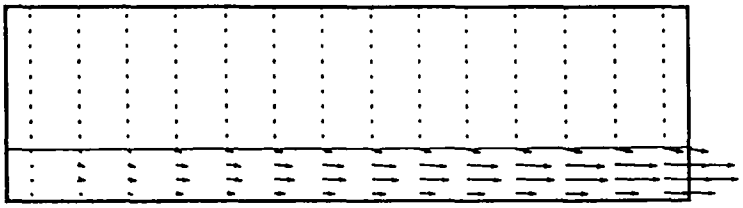

(a) t=8x10^{-6}, δ=4.442x10^{-4}

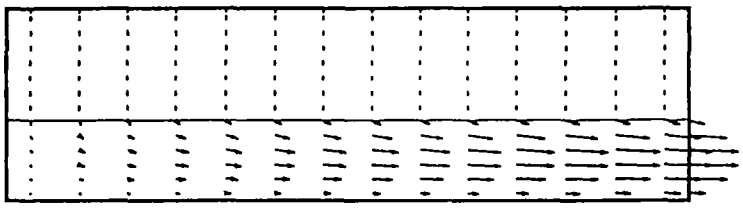

(b) t=2x10^{-5}, δ=6.820x10^{-4}

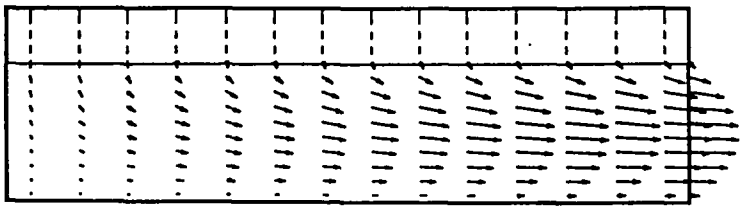

(c) t=2x10^{-4}, δ=1.055x10^{-3}

FIG. 5. Velocity vectors and the liquid–solid interface (Case A); (a) $t = 8 \times 10^{-6}$, $\delta = 4.442 \times 10^{-4}$; (b) $t = 2 \times 10^{-5}$, $\delta = 6.820 \times 10^{-4}$; (c) $t = 2 \times 10^{-4}$, $\delta = 1.055 \times 10^{-3}$.

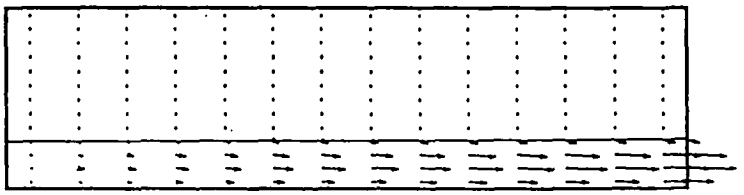

(a) t=3.2x10^{-7}, δ=7.787x10^{-4}

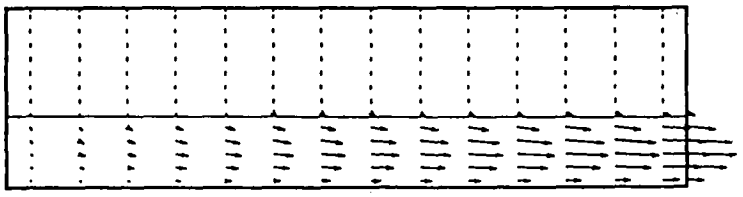

(b) t=8x10^{-7}, δ=1.183x10^{-3}

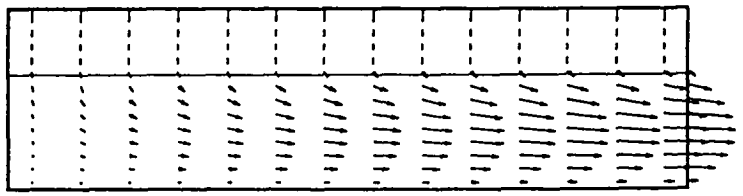

(c) t=8x10^{-6}, δ=1.785x10^{-3}

FIG. 6. Velocity vectors and the liquid–solid interface (Case B); (a) $t = 3.2 \times 10^{-7}$, $\delta = 7.787 \times 10^{-4}$; (b) $t = 8 \times 10^{-7}$, $\delta = 1.183 \times 10^{-3}$; (c) $t = 8 \times 10^{-6}$, $\delta = 1.785 \times 10^{-3}$.

layer along the flow direction gradually increases in thickness, but the difference between the minimum near the center line and the maximum near the exit is less than only 0.1%.

The timewise variation of the average thickness of liquid layer is shown in Fig. 7 in a non-dimensional form. In this figure, the thickness evaluated by the steady state analysis [5, 17] was expressed. It is clear that the system in computation approaches the steady state as time proceeds and the thickness is on the whole in good agreement with that by the previous steady state method.

Figure 8 shows the heat transferred from the heating plate and the latent and sensible heat absorbed in the phase change material, where the heat transfer rate is transformed in a dimensionless form scaled by $k(T_w - T_m)$.

The apparent velocity of solid phase and the melting rate are shown in Fig. 9 in a non-dimensional form. In the present work, the direction of the melting rate was taken as the opposite direction of the solid move-

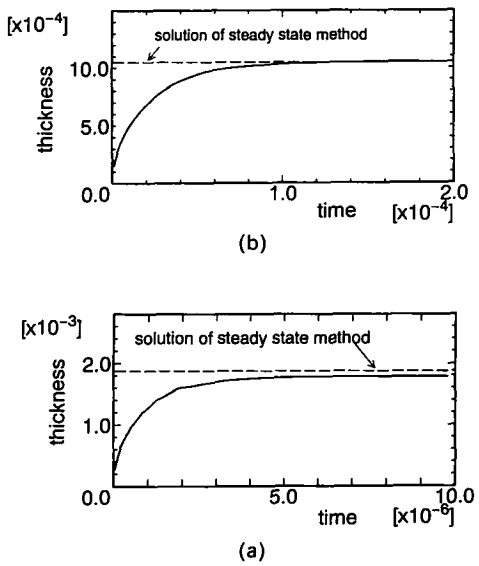

FIG. 7. Timewise variation of the average thickness of the liquid layer (problem 1); (a) Case A, (b) Case B.

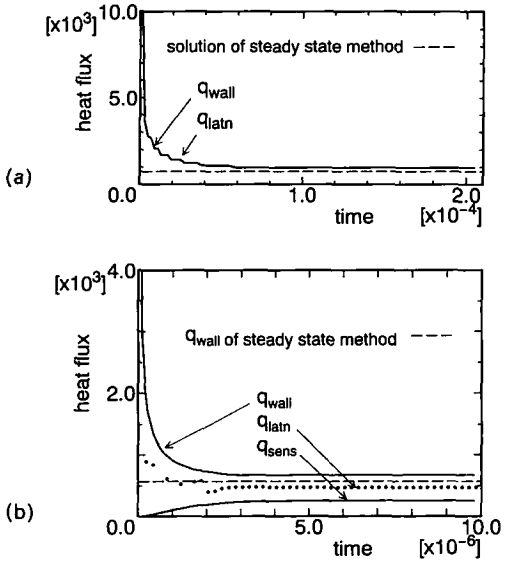

FIG. 8. Timewise variation of the heat transfer rates (q_{wall}: heat transferred from the heating plate, q_{latn}: latent heat, q_{sens}: sensible heat) (problem 1); (a) Case A, (b) Case B.

ment for convenience, instead of the normal direction of the liquid–solid interface.

In direct contact melting, the steady state generally means the situation that the velocity of solid phase becomes equal to the melting rate. Accordingly, it is found that Fig. 9 completely shows such a behavior by passing the transient process from the initial state with the solid velocity of zero and the melting rate of infinity.

Concluding remarks. It is noted through Figs. 6–9, that the system in computation approaches the steady state passing the transient process. Moreover, it is emphasized that the thickness of the liquid layer,

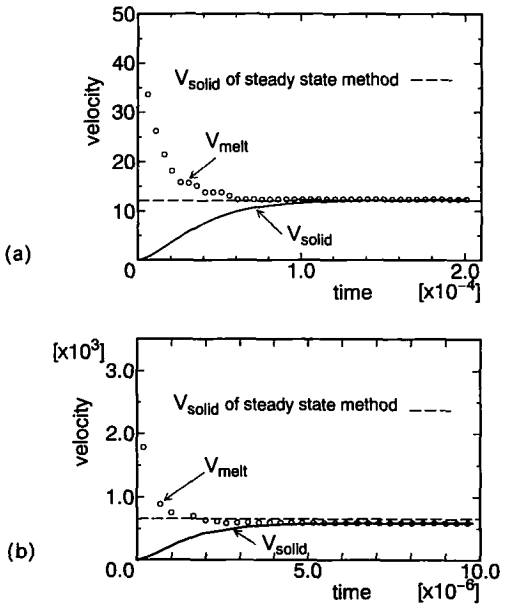

FIG. 9. Timewise variation of the apparent velocity of solid and the melting rate (problem 1); (a) Case A, (b) Case B.

the heat flux through the heating plate and the velocity of solid phase in the steady state are in good agreement with those by the earlier analysis. As stated earlier, however, the steady state analysis compared here has a limitation from a viewpoint of accuracy because only the heat conduction was considered as the mechanism of heat transfer across the liquid layer. Therefore, in a region of higher *Ste* number, it is natural that the effect of heat convection begins to appear and the discrepancy between the results increases by degrees, as shown in these figures.

The heat flux through the heating plate in Fig. 8 and the melting rate in Fig. 9 have very large values at the early stage immediately after the melting starts. The reason is that the liquid layer is extremely thin and, consequently the thermal resistance across the layer becomes significantly small. As is well known, it is seen that in the lower *Ste* number as shown in Fig. 8(a), the heat transferred from the heating plate is mainly consumed in melting, i.e. the latent heat, but in the higher *Ste* number, the ratio of sensible heat increases markedly.

Summarizing the above, it is assured that the present methodology has sufficient validity and accuracy in calculating the transient direct contact melting problem.

Test problem 2

Problem description. The second test problem, deals with a kind of a conjugate problem, shown schematically in Fig. 10 which is not proportional to the actual size and exaggerated in the region of PCM.

In this problem, the heating plate is regarded as a copper block whose initial temperature is maintained at T_w. The boundary conditions were as depicted in Fig. 10 and the copper block is insulated except at the surface contacting with the phase change material.

The melting situation is almost the same as that of the former test problem, but owing to the insulation of the heating plate, the surface temperature of the heating plate becomes lower and lower as melting proceeds. Furthermore, no assumptions for the reducing height of solid phase were different from the test problem 1.

We treated this problem in a dimensional form since the surface temperature of the heating plate, usually used in Stefan number, does change with time. Even though the initial temperature of copper block is used in place of surface temperature, it could not have a role to characterize the system at all.

The grid system is shown in Fig. 11. Total grid number is 13×24; spaced in the x-direction similar to problem 1, but divided into two regions in the y-direction, i.e. the copper block and the PCM were equally divided into 12 grids, respectively.

A number of calculations were carried out changing the initial temperature and the height of copper block. In the present paper, only one result will be reported; the specification of copper block is 0.1 m in half width and 0.05 m in height and its initial temperature is

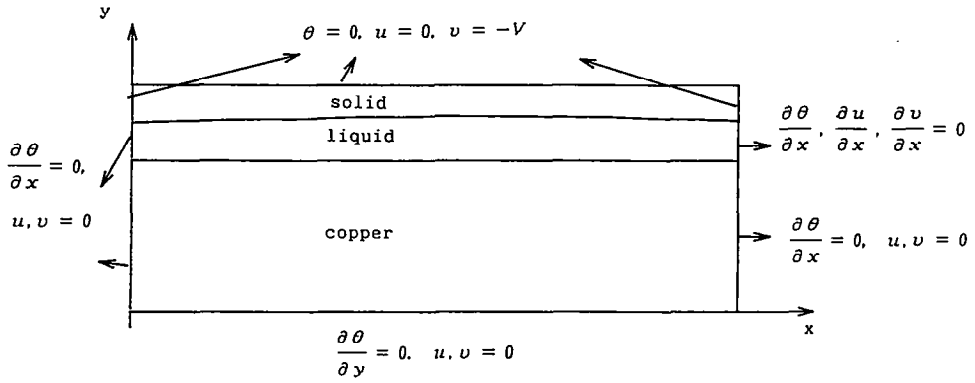

FIG. 10. Sketch of problem 2 and the boundary conditions.

20°C, and the solid phase of 0.1 m in height remains at melting temperature 0°C.

Results. The velocity field in the liquid layer showed the same pattern as that in problem 1, as shown in Figs. 5 and 6, and is omitted here. Nevertheless, the thickness of liquid layer along the flow direction is somewhat different from that in problem 1. It is in the same pattern as it increases in the flow direction and shows its maximum value at the exit. However, the thickness discrepancy between the minimum and maximum is by far a greater amount than that in problem 1 and amounts to about 4.5% although it changes with time.

The reason is obviously the fact that the surface temperature of the heating plate varies along the surface and, accordingly, the heat flux normal to the liquid layer also varies along the surface. The temperature distribution in the copper block is shown in Fig. 12. From the figure, it is found that the extent of non-uniformity of surface temperature increases with time, which makes the variation of thickness more remarkable.

Figure 13 shows the timewise variation of the average thickness. The thickness increases relatively fast as shown in problem 1 until its peak and decreases very slowly after the peak, which is caused by the reducing surface temperature.

The heat transferred from the copper block q_{wall}, the latent heat q_{latn} and sensible heat q_{sens} absorbed into the PCM, and the heat extracted from the copper block q_{cool} are depicted in Fig. 14 as the melting proceeds. Although q_{cool} should be theoretically equal to q_{wall}, it was compared in order to verify the accuracy of the calculation.

The timewise variation of velocity is shown in Fig. 15. The melting rate corresponding to q_{latn} slightly undulates in earlier stage after melting starts.

Concluding remarks. The test problem shows that the present methodology can be applied to a rather complicated problem and clearly reveals the transient process of direct contact melting.

From a standpoint of the accuracy of calculation, it can be asserted that q_{wall} and q_{cool} are nearly overlapped and they denote a summation of q_{latn} and q_{sens}. On the other hand, the undulation of q_{latn} appears partially, which may be attributed to the fact that the melting rate slightly varies with the location of the liquid–solid interface placed in a cell even under the same condition. In addition, from the analysis about the overall heat balance integrated through the entire calculation time, the integrated quantity of q_{wall} differs only by 0.1% from the summation of those of q_{latn} and q_{sens}, but the difference between q_{wall} and q_{cool} amounts to 5%.

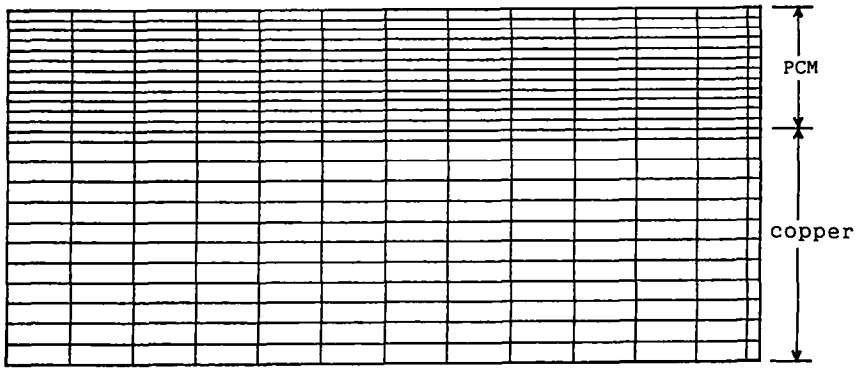

FIG. 11. Grid system of problem 2.

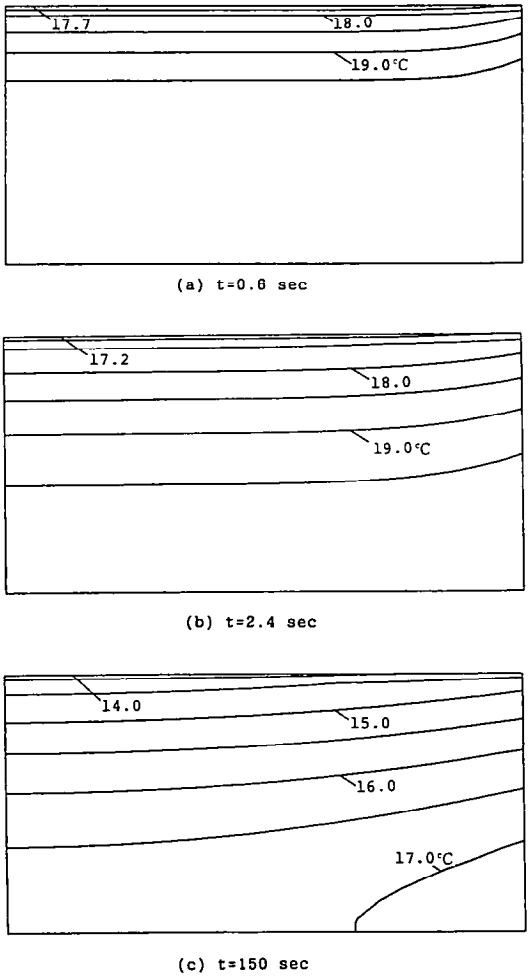

FIG. 12. Temperature distribution in the copper block (problem 2); (a) $t = 0.6$ s, (b) $t = 2.4$ s, (c) $t = 150$ s.

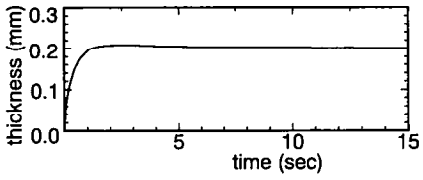

FIG. 13. Timewise variation of the average thickness of the liquid layer (problem 2).

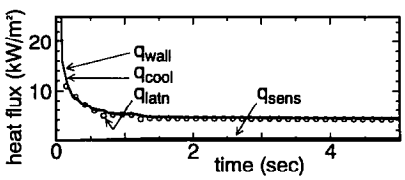

FIG. 14. Timewise variation of the heat transfer rates (q_{wall}: heat transferred from the heating plate, q_{latn}; latent heat, q_{sens}: sensible heat, q_{cool}: heat extracted for copper block) (problem 2).

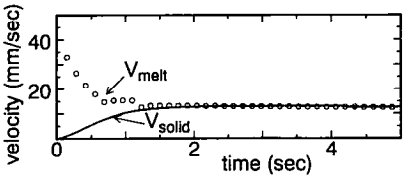

FIG. 15. Timewise variation of the apparent velocity of solid and the melting rate (problem 2).

It can be summarized that the tendency of the heat transfer and the velocity does not contradict the physical situation and the accuracy of the computation is good enough to have a reliability in an engineering sense. Above all, it should be emphasized that test problem 2 was solved with a simplicity and a feasibility in spite of a complicated situation.

CONCLUSION

The main purpose of the present work is to provide a solution for the transient behavior of the direct contact melting process. To treat easily and reasonably a matter related to an unknown velocity of solid phase at each time step was the key in solving the present moving boundary problem. The validity of the present method was examined through test problem 1 and the applicability to a wide range of problems was tested through test problem 2.

In conclusion, the present method can be utilized in comprehending the transient behavior of direct contact melting and also can be applied to a variety of the problems, which accompany the phase change with moving body. Improvements in the present method will continue in the future with respect to the efficiency and the accuracy.

REFERENCES

1. A. Saito, Y. Utaka, M. Akiyoshi and K. Katayama, On the contact heat transfer with melting (1st report, experimental study), *Bull. JSME* **28**(240), 1142–1149 (1985). (Translated from *Trans. JSME(B)* **50**(458), 2393–2400 (1984).)
2. A. Saito, Y. Utaka, M. Akiyoshi and K. Katayama, On the contact heat transfer with melting (2nd report, analytical study), *Bull. JSME* **28**(242), 1703–1709 (1985). (Translated from *Trans. JSME(B)* **50**(460), 2977–2984 (1984).)
3. A. Saito, Y. Utaka and Y. Tokihiro, On contact heat transfer with melting (3rd report, the melting on the inner surface of a horizontal cylindrical tube), *JSME Int. J.* **31**(1), Ser. 2, 58–65 (1988). (Translated from *Trans. JSME(B)* **53**(491), 2130–2136 (1984).)
4. M. Bareiss and H. Beer, An analytical solution of the heat transfer process during melting of an unfixed solid phase change material inside a horizontal tube, *Int. J. Heat Mass Transfer* **27**, 739–745 (1984).
5. M. K. Moallemi, B. W. Webb and R. Viskanta, An experimental and analytical study of close-contact melting, *J. Heat Transfer* **108**, 894–899 (1986).
6. M. K. Moallemi and R. Viskanta, Analysis of close-contact melting heat transfer, *Int. J. Heat Mass Transfer* **29**, 855–867 (1986).
7. E. M. Sparrow and G. T. Geiger, Melting in a horizontal tube with the solid either constrained or free to fall under gravity, *Int. J. Heat Mass Transfer* **29**, 1007–1019 (1986).

8. A Saito, H. K. Hong and O. Hirokane, Heat transfer enhancement in the direct contact melting process, *Int. J. Heat Mass Transfer* **35**, 295–305 (1992).
9. E. M. Sparrow, S. V. Patankar and S. Ramadhyani, Analysis of melting in the presence of natural convection in the melt region, *J. Heat Transfer* **99**, 520–526 (1978).
10. A. Gadgil and D. Gobin, Analysis of two-dimensional melting in rectangular enclosures in presence of convection, *J. Heat Transfer* **106**, 12–19 (1984).
11. V. R. Voller and C. Prakash, A fixed grid numerical modeling methodology of convection/diffusion mushy phase change problems, *Int. J. Heat Mass Transfer* **30**, 1709–1719 (1987).
12. A. D. Brent, V. R. Voller and K. J. Reid, Enthalpy-porosity technique for modeling convection-diffusion phase change: Application to the melting of a pure metal, *Numer. Heat Transfer* **13**, 297–318 (1988).
13. M. Lacroix and V. R. Voller, Finite difference solutions of solidification phase change problems: transformed versus fixed grids, *Numer. Heat Transfer* (Part B) **17**, 25–41 (1990).
14. D. K. Gartling, Finite element analysis of convection heat transfer problems with change of phase. In *Computer Methods in Fluids* (Edited by K. Morgan *et al.*), pp. 257–284. Pentech, London (1980).
15. J. P. Van Doormaal and G. D. Raithby, Enhancements of the SIMPLE method for predicting incompressible fluid flows, *Numer. Heat Transfer* **7**, 147–163 (1984).
16. C. W. Hirt and B. D. Nichols, Volume of fluid (VOF) method for the dynamics of free boundaries, *J. Comput. Phys.* **39**, 201–225 (1981).
17. A Saito, Y. Utaka, K. Shonoda and K. Katayama, Basic research on the latent heat thermal energy storage utilizing the contact melting phenomena, *Bull. JSME* **29**(255), 2946–2952 (1986), (*Trans. JSME B* **52**(473), 110–116 (1986)).